# Power Controlled Soliton Stability and Steering in Lattices with Saturable Nonlinearity

Ljupčo Hadžievski
*Vinča Institute of Nuclear Sciences, P.O. Box 522, 11001 Belgrade, Serbia and Montenegro*

Aleksandra Maluckov
*Faculty of Sciences and Mathematics, University of Niš, 18000 Niš, Serbia and Montenegro*

Milutin Stepić and Detlef Kip
*Institute of Physics and Physical Technologies, Technical University of Clausthal, D-38678 Clausthal-Zellerfeld, Germany*
(Received 12 December 2003; published 12 July 2004)

Dynamical properties of discrete solitons in nonlinear Schrödinger lattices with saturable nonlinearity are studied in the framework of the one-dimensional discrete Vinetskii-Kukhtarev model. Two stationary strongly localized modes, centered on site ($A$) and *between* two neighboring sites ($B$), are obtained. The associated Peierls-Nabarro potential is bounded and has multiple zeros indicating strong implications on the stability and dynamics of the localized modes. Besides a stable propagation of mode $A$, a stable propagation of mode $B$ is also possible. The enhanced ability of the large power solitons to move across the lattice is pointed out and numerically verified.

DOI: 10.1103/PhysRevLett.93.033901 PACS numbers: 42.65.Tg, 42.65.Wi, 42.82.Et, 63.20.Pw

Nonlinear discrete systems are recognized in various fields of physics. The energy transport in molecular chains [1], optical pulse propagation in waveguide arrays [2], Scheibe aggregates [3], arrays of Josephson junctions [4], mixed-valence transition metal complexes [5], the motion of localized waves on discrete electrical lattices [6], coupled arrays of nonlinear mechanical pendulums [7], and photonic crystal waveguides [8] are only some of the well-known examples from this realm. All of these share the common phenomenon of nonlinear wave localization giving rise to the existence of intrinsic localized modes such as discrete solitons. The most interesting and extensively studied are optical discrete solitons in nonlinear waveguide lattices (see recent review articles [9]) because of their potential applications in designing ultimate fast all-optical devices. The fundamental concept of *light guiding light* can be achieved using dynamical properties of the optical discrete solitons and their interactions. A standard theoretical approach for the description of lattices which consist of equally spaced identical nonlinear lattice elements is based on the decomposition of the total field in a sum of weakly coupled modes exited in each of the waveguides of the lattice. This approach, known as a tight-binding approximation, often leads to different versions of the discrete nonlinear Schrödinger (DNLS) equation. Discrete systems with cubic (Kerr) nonlinearity, such as the waveguide array in AlGaAs [10] are well described by the cubic DNLS equation. It is shown on the example of the one-dimensional (1D) DNLS lattice that, for a given power, two stationary localized modes exist [11]: one stable ($A$) centered on a waveguide and one unstable ($B$) centered *between* two neighboring waveguides. The existence and stability of modes $A$ and $B$ for the case of the coupled DNLS model describing transport of the vibrational energy in crystalline acetanilide are discussed in [12]. The difference of their energies is attributed to the Peierls-Nabarro (PN) effective periodic potential generated by the lattice discreteness, originally introduced in the theory of crystal dislocations [13]. The obtained PN potential is always negative and proportional to the soliton power. The power dependent soliton steering [9,10,14,15] is explained with the PN potential assuming it as the minimum barrier which must be overcome to propagate a soliton across the nonlinear lattice [10,11].

The aim of this Letter is to demonstrate that the dynamical properties of the DNLS lattices with saturable nonlinearity, such as optical waveguides in photorefractive crystals, differ considerably from those of the discrete lattices with cubic (Kerr) nonlinearity. This strongly affects the soliton's stability properties and its propagation across the lattice. Similar effects in a quantum DNLS model are studied in a very recent paper [16].

We begin our study with the 1D DNLS lattice model with saturable nonlinearity, which represents a discrete version of the Vinetskii-Kukhtarev equation [17]

$$i\frac{\partial U_n}{\partial z} + K(U_{n+1} + U_{n-1} - 2U_n) - \beta\frac{U_n}{1 + |U_n|^2} = 0. \tag{1}$$

Here $U_n$ is the wave function in the $n$th lattice element ($n = 1, \ldots, N$) with ($U_{N+1} = U_1$) for the case of periodic boundary conditions, $K$ is the coupling constant, and $\beta$ is the nonlinearity parameter.

The above equation represents a system of linearly coupled nonlinear differential equations which are not integrable in the general case but possess two conserved quantities: Hamiltonian $H = \sum_n[\beta\ln(1 + |U_n|^2) + K|U_{n-1} - U_n|^2]$ and the number of quanta (power) $P = \sum_n|U_n|^2$.

 © 2004 The American Physical Society 

The exact lattice independent constant amplitude solution of Eq. (1),

$$U_n = \sqrt{\frac{\beta - \nu}{\nu}} \exp(-i\nu z), \quad (2)$$

is unstable with respect to small modulations. Assuming perturbations $\delta U_n \propto e^{-i\Omega z} \ll U_n$, the linear stability analysis yields the dispersion relation

$$\Omega^2 = 8K\sin^2(\pi/N)[2K\sin^2(\pi/N) - \nu(1 - \nu/\beta)], \quad (3)$$

which for $\Omega^2 < 0$ defines the following instability frequency band:

$$\nu \in [2K\sin^2(\pi/N), \beta - 2K\sin^2(\pi/N)]. \quad (4)$$

This process of modulation instability is responsible for energy localization and creation of discrete solitons. Such stationary localized modes can be obtained from Eq. (1) by assuming solutions in the form $U_n(z) = Ff_n e^{-i\nu z}$ and a set of coupled algebraic equations for the real function $f_n$,

$$\nu f_n + K(f_{n+1} + f_{n-1} - 2f_n) - \frac{\beta f_n}{1 + F^2|f_n|^2} = 0. \quad (5)$$

Equation (5) gives two types of strongly localized modes. The first one ($A$) centered at the lattice site $n = 0$, assuming $F = A$, $f_0 = 1$, $f_{-n} = f_n$, has a pattern in the form

$$U_n^{(A)}(z) = A(\ldots, f_2^A, f_1^A, 1, f_1^A, f_2^A, \ldots)e^{-i\nu z}, \quad (6)$$

where the lattice sites are indexed with $n = 0, \pm1, \pm2, \ldots$.

For the strongly localized modes satisfying $|f_{n+1}| \ll |f_n|$ for $n \geq 0$, we can consider a linear propagation in the lattice elements with $|n| > 1$, and the total power $P$ and Hamiltonian $H$ can be approximately calculated as

$$P_A = A^2 \frac{(\gamma + 2 - \omega)^2 + 1}{(\gamma + 2 - \omega)^2 - 1},$$
$$H_A = \gamma \ln(1 + A^2) + 2\gamma \ln\left[\prod_{j=1}^{\infty}\left(1 + \frac{A^2}{(\gamma + 2 - \omega)^{2j}}\right)\right]$$
$$+ 2A^2 \frac{(\gamma + 1 - \omega)^2}{(\gamma + 2 - \omega)^2 + 1}, \quad (7)$$

where $\gamma = \beta/K$, $\omega = \nu/K$, and the soliton amplitude $A$ is defined by

$$A^2 = \frac{(\gamma + 2 - \omega)^2 - 2}{(\gamma + 2 - \omega)(\omega - 2) + 2}. \quad (8)$$

The second strongly localized mode ($B$) centered *between* two neighboring lattice elements $n = \pm1$, assuming $F = B$, $f_{\pm1} = 1$, $f_{-n} = f_n$, has a pattern in the form

$$U_n^{(B)}(z) = B(\ldots, f_3^B, f_2^B, 1, 1, f_2^B, f_3^B, \ldots)e^{-i\nu z}, \quad (9)$$

where the lattice sites are indexed with $n = \pm1, \pm2, \ldots$.

With a similar procedure as applied for the mode $A$, under the assumption $|f_{n+1}| \ll |f_n|$ for $n \geq 1$, we can approximately calculate the total power $P$ and Hamiltonian $H$ for the mode $B$,

$$P_B = 2B^2 \frac{(\gamma + 2 - \omega)^2}{(\gamma + 2 - \omega)^2 - 1},$$
$$H_B = 2\gamma \ln\left[\prod_{j=0}^{\infty}\left(1 + \frac{B^2}{(\gamma + 2 - \omega)^{2j}}\right)\right]$$
$$+ 2B^2 \frac{(\gamma + 1 - \omega)^2}{(\gamma + 2 - \omega)^2 + 1}, \quad (10)$$

and the corresponding soliton amplitude

$$B^2 = \frac{(\gamma + 2 - \omega)(\gamma + 1 - \omega) - 1}{(\gamma + 2 - \omega)(\omega - 1) + 1}. \quad (11)$$

The difference in energy between these two stationary localized states for the same power level $P_A = P_B = P$ defines the effective PN potential [10,11]

$$\Delta E_{AB}(P) = H_A(P) - H_B(P). \quad (12)$$

The curve $\Delta E_{AB}(P)$, which is presented in Fig. 1 by a solid line, shows that the effective PN potential changes its sign for a critical power $P_{c1}$, which brings important implications on the stability properties of the localized modes ($A$ and $B$) and soliton steering across the lattice elements. In the region $0 < P < P_{c1}$ mode $A$ has a lower energy than mode $B$ ($H_A < H_B$) for the same power $P$, indicating that mode $A$ is stable and mode $B$ is unstable. For this lower power region this coincides with the results obtained in [10,11] for the DNLS lattices with a Kerr nonlinearity. The obtained agrement is expected because in the small amplitude limit Eq. (1) reduces to the cubic DNLS equation. However, in the region $P > P_{c1}$ the situation is the opposite ($H_A > H_B$): mode $B$ is stable and mode $A$ is unstable. It means, contrary to the

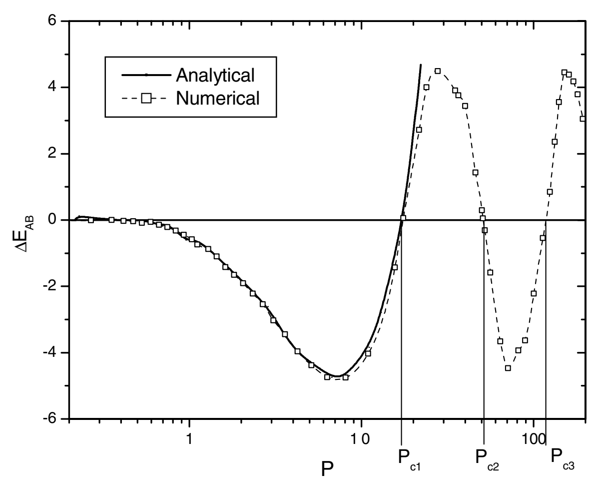


FIG. 1. Analytically (solid line) and numerically calculated PN potential versus soliton power $P$ for discrete lattices with $\beta = 18.2$ and $K = 2$.

DNLS lattices with cubic nonlinearity [10,11], a stable propagation of the discrete soliton centered *between* the neighboring lattice elements ($B$) is possible. The critical power $P_{c1}$, i.e., a zero of the PN potential, represents marginally stable states for both modes.

The observed PN potential can be explained by a cascade nature of amplitude saturation in the lattice elements. The amplitude of the central element for mode $A$ increases with increasing power level $P$ up to a point when it reaches the saturation level. A further increase of $P$ is the result of increasing amplitudes in two neighboring lattice elements ($n = \pm 1$). Consecutively, when the amplitudes in the lattice elements ($n = \pm 1$) saturate, the amplitudes of the next lattice elements ($n = \pm 2$) contribute to the further increase of $P$. This cascade process continues with increasing of $P$, while mode $A$ becomes less and less localized. The same process takes place also for mode $B$ but for larger values of $P$ because two lattice elements saturate simultaneously. The numerically obtained power dependence of the amplitude in the central and two neighboring elements for both modes, shown in Fig. 2, clearly illustrates the cascade nature of the saturation. This means that increasing $P$ does not lead to a continuous energy localization into a single lattice element and decoupling from the rest of the lattice as in the case of the DNLS lattice with cubic nonlinearity. Instead, the described cascade saturation takes place and suppresses an energy localization resulting in the existence of less and less localized modes as $P$ increases. However, this explanation indicates the existence of a bounded PN potential with multiple zeros. The numerically obtained PN potential, shown in Fig. 1 by a dashed line, confirms our predictions. A bounded PN potential with multiple zeros ($P_{c1}, P_{c2}, P_{c3}, \ldots$) is obtained, where $P_{c1}$ coincides with the analytically predicted value. The other zeros cannot be obtained by the described analytical approach since the assumption $|f_{n+1}| \ll |f_n|$ used for deriving the analytical expressions (7) and (10), fails for large $P$.

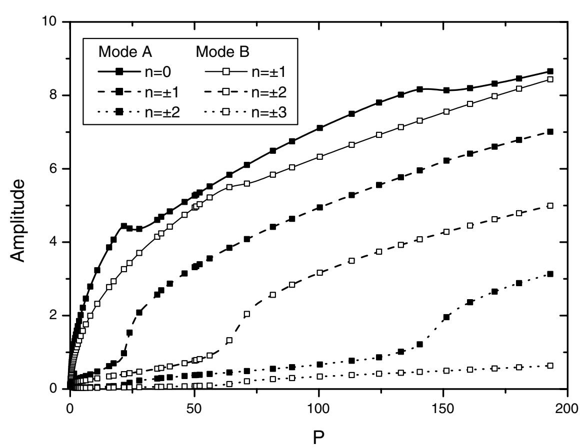


FIG. 2. Amplitude in the central lattice element and its neighbors for both localized modes as a function of soliton power $P$ for discrete lattices with $N = 101$, $\beta = 18.2$, and $K = 2$.

According to the scenario described in Refs. [10,11] that the two modes $A$ and $B$ can be approximately viewed as dynamical states of the same moving localized mode, one can expect that the shape of the PN potential strongly affects the power dependent soliton steering across the lattice elements. The boundedness of the PN potential barrier brings the general conclusion that the ability of large power solitons to move across the lattice is considerably higher than in the case of DNLS lattices with cubic nonlinearity. The large power solitons forced to move sideways may propagate or may be trapped inside the potential barrier exhibiting oscillations of the soliton velocity. Moreover, the existence of zeros of the PN potential indicates the possibility for the existence of unlimited soliton steering across the lattice. However, modes $A$ and $B$ represent pure solitons without internal oscillations but with different self-frequencies ($\omega_A$, $\omega_B$) for the fixed power $P$. During the periodic transition of the moving mode through modes $A$ and $B$, the self-frequency oscillates between $\omega_A$ and $\omega_B$. Therefore, the moving modes are not pure solitons but breathers with an additional internal mode of freedom. In spite of this, we can conclude that the PN barrier is only one among other factors that could influence the mobility effect.

In order to verify our analytical results for the stability of the modes $A$ and $B$, as well as to estimate the influence of the PN potential barrier on the mobility of the solitons across the lattice elements, we have performed a set of numerical simulations of Eq. (1), based on the sixth order Runge-Kutta procedure with regular checking of the conserved quantities $P$ and $H$. In the regions with negative PN potential barrier we observe a stable propagation of mode $A$, while the unstable mode $B$ quickly relaxes into the stable mode $A$. In the regions with positive PN potential barrier we observe a stable propagation of mode $B$ [Fig. 3(a)], while the unstable mode $A$ quickly relaxes into the stable mode $B$. For the critical power ($P_{c1}, P_{c2}, P_{c3}, \ldots$) we observe propagation of both modes.

Solitons are numerically forced to move sideways by the introduction of a small phase difference tilt between adjacent lattice elements. The observed dynamics is complex and strongly depends on soliton power and introduced phase difference. Results confirm our conclusion that a moving mode is a breather type, and also our prediction of the enhanced mobility of large power solitons. Here, to illustrate our conclusions, we present a few of the most instructive examples. We launch large power solitons with $P = 21.63 > P_{c1}$, where mode $A$ is unstable and mode $B$ is stable (opposite situation than for the DNLS lattices with cubic nonlinearity). The corresponding example of stable propagation of mode $B$ is shown in Fig. 3(a). Soliton steering can be initiated from unstable mode $A$ by introducing a small phase difference. This is consistent with the experiments with DNLS lattices with

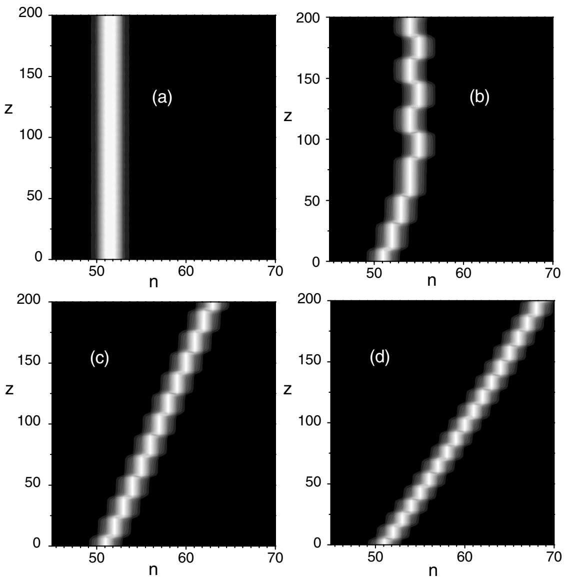


FIG. 3. Illustration of the soliton dynamics with $P = 21.63$ in the lattice with $N = 101$, $\beta = 18.2$, and $K = 2$. (a)–(d) represent gray scale maps of the intensity profiles over the lattice for (a) stable propagation of the mode $B$, and soliton steering initiated from mode $A$ with different initial phase differences: (b) $\alpha = 0.0027$, (c) $\alpha = 0.005$, and (d) $\alpha = 0.0155$.

cubic nonlinearity [10] where the soliton steering is initiated from mode $B$.

The introduced phase difference increases the $H$ and as a result we get an initial state with the same $P$ but with $H$ above the $H_A$ of the unstable mode ($A$). As a consequence of the conservation of $P$ and $H$, the energy difference is transferred partly into the exited internal mode of freedom and partly into the kinetic energy enabling soliton steering across the lattice. Figures 3(b)–3(d) demonstrate the propagation of solitons across the lattice for three values of the initial phase difference. The soliton with a small initial phase difference [Fig. 3(b)] starts to steer, slows down, and is finally trapped by the potential barrier composing a complex breather-type localized mode where the energy mainly oscillates between two lattice elements. Solitons with a larger initial phase difference propagate across the lattice with a constant transverse velocity [Fig. 3(c)]. Further increasing of the initial phase difference induces soliton steering with a larger transverse velocity [Fig. 3(d)].

In conclusion, we have shown on the example of a 1D model that dynamical properties of DNLS lattices with saturable nonlinearity differ considerably from those of the DNLS lattices with cubic nonlinearity. The most important difference is the existence of stable discrete solitons centered *between* two neighboring lattice elements (mode $B$) resulting in an enhanced ability for soliton steering across the lattice. These properties are power dependent and can be of interest for developing new ideas for designing all-optical routing and switching devices. We further expect that these results will be experimentally confirmed with the waveguide lattices fabricated in photorefractive crystals like strontium-barium niobate (SBN61, $Sr_{0.61}Ba_{0.39}Nb_2O_6$). Currently we are developing such 1D waveguide arrays in SBN using He ion implantation and photoresist patterning of the channels.

The authors thank M. M. Škorić for many useful discussions. This work is supported by Ministry of Science, Development and Technologies of Republic Serbia (Project No. 1964), by German Federal Ministry of Education and Research (BMBF, Grant No. DIP-E6.1), and by INTAS (Contract No. 01-0481).

[1] W. P. Su, J. R. Schrieffer, and A. J. Heeger, Phys. Rev. Lett. **42**, 1698 (1979).
[2] D. N. Christodoulides and R. I. Joseph, Opt. Lett. **13**, 794 (1988).
[3] P. L. Christiansen, O. Bang, S. Pagano, and G. Vitiello, Nanobiology **1**, 229 (1992).
[4] E. Trias, J. J. Mazo, and T. P. Orlando, Phys. Rev. Lett. **84**, 741 (2000).
[5] B. I. Swanson, J. A. Brozik, S. P. Love, G. F. Strouse, A. P. Shreve, A. R. Bishop, W. Z. Wang, and M. I. Salkola, Phys. Rev. Lett. **82**, 3288 (1999).
[6] P. Marquie, J. M. Bilbault, and M. Remoissenet, Phys. Rev. E **51**, 6127 (1995).
[7] B. Denardo, B. Galvin, A. Greenfield, A. Larraza, S. Putterman, and W. Wright, Phys. Rev. Lett. **68**, 1730 (1992).
[8] S. F. Mingaleev, Yu. S. Kivshar, and R. A. Sammut, Phys. Rev. E **62**, 5777 (2000); A. A. Sukhorukov and Y. S. Kivshar, Phys. Rev. Lett. **87**, 083901 (2001); J. W. Fleischer, M. Segev, N. K. Efremidis, and D. N. Christodoulides, Nature (London) **422**, 147 (2003).
[9] G. I. A. Stegeman, D. N. Christodoulides, and M. Segev, IEEE J. Sel. Top. Quantum Electron. **6**, 1419 (2000); A. Sukhorukov, Y. S. Kivshar, H. S. Eisenberg, and Y. Silberberg, IEEE J. Quantum Electron. **39**, 31 (2003); D. N. Christodoulides, F. Lederer, and Y. Silberberg, Nature (London) **424**, 817 (2003).
[10] R. Morandotti, U. Peschel, J. S. Aitchison, H. S. Eisenberg, and Y. Silberberg, Phys. Rev. Lett. **83**, 2726 (1999).
[11] Yu. S. Kivshar and D. K. Campbell, Phys. Rev. E **48**, 3077 (1993).
[12] J. C. Eilbeck, P. S. Lomdahl, and A. C. Scott, Phys. Rev. B **30**, 4703 (1984).
[13] R. F. Peierls, Proc. R. Soc. London **52**, 34 (1940); F. R. Nabbaro, *ibid.* **59**, 256 (1947).
[14] A. B. Aceves, C. De Angelis, T. Peschel, R. Muschall, F. Lederer, S. Trillo, and S. Wabnitz, Phys. Rev. E **53**, 1172 (1996).
[15] H. Feddersen, in *Nonlinear Sructures in Physics and Biology*, edited by M. Remoissenet and M. Peyrard (Springer-Verlag, Berlin, 1991), p. 159
[16] J. Dorignac, J. C. Eilbeck, M. Salerno, and A. C. Scott, quant-ph 0312143.
[17] V. O. Vinetskii and N. V. Kukhtarev, Sov. Phys. Solid State **16**, 2414 (1975).